

RESEARCH ARTICLE

Neuromuscular control of hovering wingbeat kinematics in response to distinct flight challenges in the ruby-throated hummingbird, *Archilochus colubris*

Sajeni Mahalingam* and Kenneth C. Welch, Jr[†]

Department of Biological Sciences, University of Toronto Scarborough, Toronto, ON, Canada, M1C 1A4 and Department of Cell and Systems Biology, University of Toronto, Toronto, ON, Canada, M5S 3G5

*Present address: Department of Biology, McMaster University, Hamilton, ON, Canada, L8S 4L8

[†]Author for correspondence (kwelch@utsc.utoronto.ca)

SUMMARY

While producing one of the highest sustained mass-specific power outputs of any vertebrate, hovering hummingbirds must also precisely modulate the activity of their primary flight muscles to vary wingbeat kinematics and modulate lift production. Although recent studies have begun to explore how pectoralis (the primary downstroke muscle) neuromuscular activation and wingbeat kinematics are linked in hummingbirds, it is unclear whether different species modulate these features in similar ways, or consistently in response to distinct flight challenges. In addition, little is known about how the antagonist, the supracoracoideus, is modulated to power the symmetrical hovering upstroke. We obtained simultaneous recordings of wingbeat kinematics and electromyograms from the pectoralis and supracoracoideus in ruby-throated hummingbirds (*Archilochus colubris*) hovering under the following conditions: (1) ambient air, (2) air density reduction trials, (3) submaximal load-lifting trials and (4) maximal load-lifting trials. Increased power output was achieved through increased stroke amplitude during air density reduction and load-lifting trials, but wingbeat frequency only increased at low air densities. Overall, relative electromyographic (EMG) intensity was the best predictor of stroke amplitude and is correlated with angular velocity of the wingtip. The relationship between muscle activation intensity and kinematics was independent of treatment type, indicating that reduced drag on the wings in hypodense air did not lead to high wingtip angular velocities independently of increased muscle work. EMG bursts consistently began and ended before muscle shortening under all conditions. During all sustained hovering, spike number per burst consistently averaged 1.2 in the pectoralis and 2.0 in the supracoracoideus. The number of spikes increased to 2.5–3 in both muscles during maximal load-lifting trials. Despite the relative kinematic symmetry of the hovering downstroke and upstroke, the supracoracoideus was activated ~1 ms earlier, EMG bursts were longer (~0.9 ms) and they exhibited 1.6 times as many spikes per burst. We hypothesize that earlier and more sustained activation of the supracoracoideus fibres is necessary to offset the greater compliance resulting from the presence of the supracoracoid tendon.

Key words: Supracoracoideus, pectoralis, load-lifting, air density reduction, electromyography, flight muscles, hovering flight.

Received 12 April 2013; Accepted 31 July 2013

INTRODUCTION

Understanding how flight muscles function has been of particular interest to biologists because these muscles power the most expensive form of locomotion. Several studies have examined how wingbeat kinematics, neuromuscular activation patterns and mechanical function in the pectoralis, the primary downstroke muscle, vary with forward flight velocity (Tobalske et al., 1997; Hedrick et al., 2003; Ellerby and Askew, 2007; Tobalske et al., 2010). In agreement with recent work quantifying metabolic power input as a function of flight velocity (Tobalske et al., 2003; Ellerby and Askew, 2007), these studies have generally noted a U-shaped power curve and a similar pattern in the electromyographic (EMG) recordings, with power output and EMG intensity greatest at either velocity extreme and lowest at moderate speeds. Fewer studies have examined variation in power output or EMG activity in the primary upstroke muscle, the supracoracoideus (e.g. Tobalske et al., 1997; Tobalske and Biewener, 2008; Tobalske et al., 2010). Some studies show that variation in neuromuscular activation in the supracoracoideus as a function of flight velocity is similar to that seen in the pectoralis (Tobalske et al., 1997; Tobalske et al., 2010).

However, the difference in aerodynamic activity of the upstroke and downstroke during forward flight, as well as the fact that some birds can, with training, achieve takeoff flight without the use of the supracoracoideus (Degernes and Feduccia, 2001; Sokoloff et al., 2001), suggest that the role of the supracoracoideus in powering some flight styles is not easily predicted.

The unique flight of hummingbirds is facilitated by an upstroke that contributes much more to overall lift production than occurs in other birds during hovering. In hovering hummingbirds, lift generation during the upstroke is partly the result of (i) a stroke plane that is roughly horizontal and (ii) rotation of the wing along its long axis (Warrick et al., 2005; Warrick et al., 2009). These features contribute to a hovering wingbeat with greater kinematic symmetry than is observed in other birds (Warrick et al., 2005; Warrick et al., 2009). This kinematic symmetry implies greater similarity in mechanical power output from the muscles that power the downstroke and upstroke, the pectoralis and supracoracoideus, respectively. In addition, the supracoracoideus is larger in hummingbirds than in other birds, at approximately half the size of the pectoralis (Greenewalt, 1962; Tobalske et al., 2010). Greater

wingbeat symmetry (Warrick et al., 2005; Warrick et al., 2009) and greater morphological similarity (Greenewalt, 1962; Tobalske et al., 2010) suggest potentially greater correspondence in mechanical function and neuromuscular activation patterning between these muscles than is seen in other birds.

Laboratory investigations into the modulation of power output and wingbeat kinematics during hovering flight have traditionally imposed one of two challenges: flight in hypodense air mixtures (e.g. Chai and Dudley, 1995; Chai and Dudley, 1996; Altshuler et al., 2010b) or the lifting of additional mass (Wells, 1993). Studies have revealed variation in the kinematic strategies hummingbirds can adopt to increase power output related to differences in the nature of the challenge or possibly to differences among species. During flight in hypodense air in laboratory settings, investigators have reported that ruby-throated (*Archilochus colubris*) (Chai and Dudley, 1995; Chai and Dudley, 1996) and Anna's hummingbirds (*Calypte anna*) (Altshuler et al., 2010b) increase stroke amplitude and wingbeat frequency as air density decreases. Researchers have also reported that stroke amplitude during hovering is greater at higher elevation for species found along natural elevational gradients in the field (Altshuler et al., 2004; Altshuler and Dudley, 2003). In contrast, Wells found that broad-tailed (*Selasphorus platycercus*) and rufous hummingbirds (*S. rufus*) that lifted sub-maximal loads increased stroke amplitude but that wingbeat frequency remained constant (Wells, 1993).

Recently, there has been a resurgence of interest in the neuromuscular control of variation in power output and wingbeat kinematics during flight in hummingbirds (e.g. Altshuler et al., 2010b; Altshuler et al., 2012; Tobalske et al., 2010). Beginning in 1968 with a study by Hagiwara and colleagues and continuing more recently, investigators have reported unique EMGs from the major flight muscles consisting of one to a few discrete spikes with each wingbeat (Hagiwara et al., 1968; Altshuler et al., 2010b; Tobalske, 2010). The simple nature of the EMG waveforms in the hummingbird pectoralis has permitted unique insights into how neuromuscular control, motor unit recruitment and kinematic performance are related. Altshuler and colleagues have shown that Anna's hummingbirds achieve increased stroke amplitude in hypodense air *via* progressive spatial recruitment of pectoralis motor units, but that temporal recruitment is also required when both stroke amplitude and wingbeat frequency are dramatically increased during brief asymptotic maximal load lifting (Altshuler et al., 2010b). Tobalske et al. reported that rufous hummingbird pectoralis and supracoracoideus EMGs varied in similar ways as birds flew at a range of forward flight velocities (Tobalske et al., 2010). Nonetheless, we do not understand how variation in the neuromuscular control of the supracoracoideus during hovering flight (e.g. timing of activation, number of spikes per burst, or intensity) compares to that of the pectoralis. Additionally, it remains unclear whether differences in observed variation in wingbeat kinematics among species challenged by either submaximal load lifting or flight in hypodense air are the result of variation in motor recruitment patterns or of differences in the amount of drag the wing encounters during flight in fluids of differing density.

To address these questions we studied individual ruby-throated hummingbirds as we challenged flight performance in four distinct ways (see Fig. 1): hovering in normodense air, hovering in progressively less dense air mixtures, the sustainable lifting of progressively greater submaximal loads in normodense air, and the brief lifting of maximal loads in normodense air. During each challenge we obtained high-speed video recordings in order to determine wingbeat frequency, stroke amplitude and the mean

angular velocity of the wing tip. In addition, we simultaneously recorded EMG waveforms from both the pectoralis and supracoracoideus muscles in order to determine the number of spikes, rectified EMG area (intensity) and timing of EMG bursts relative to wingbeat transitions (i.e. pronation or supination events, respectively).

MATERIALS AND METHODS

Experimental animals

Four adult male ruby-throated hummingbirds, *Archilochus colubris* (Linnaeus 1758) were captured in Scarborough, ON, Canada. The birds were housed individually in 61×61×61 cm cages. Birds were fed Nektar Plus (Nekton, Pforzheim, Germany) *ad libitum* and were maintained on a 14h:10h light:dark cycle. Individual mass averaged 2.81±0.09 g during the experiments, determined by averaging each individual's mass measured at the beginning and at the end of the experiment. Capture of animals was accomplished under permit from the Canadian Wildlife Service in Ontario. All procedures were approved by the University of Toronto Laboratory Animal Care Committee.

Surgical procedures

Muscle activation patterning was recorded from both the pectoralis and supracoracoideus. Implantation of electrodes and approaches used in the collection of EMG activity followed protocols described elsewhere (Altshuler et al., 2010b). To accomplish electrode implantation, birds were anaesthetized using vaporized isoflurane and maintained on a heating pad. The skin above the pectoralis was cleaned with betadine solution (Purdue Pharma, Pickering, ON, Canada) and feathers were brushed aside or removed, when necessary. Two bipolar electrodes were each made from a pair of 0.08 mm diameter bifilar HML-insulated silver wires (California Fine Wire Company, Grover Beach, CA, USA). The tips of each lead in each bipolar electrode were offset by ~0.5 mm and stripped of insulation at the first 0.5 mm of each lead. The terminal ~1 mm of each electrode was inserted into a 26 gauge needle and bent 180 deg in order to form a hook. One of the bipolar electrodes was inserted into the left pectoralis muscle (Fig. 2A). Once inserted, the electrode was held in place using fine forceps, while the needle was removed. The hook at the end of the electrode kept the wire embedded in the muscle. The electrode lead was sutured (6-0, silk suture) to the skin above the pectoralis. The same procedure was followed for the implantation of the electrode into the left supracoracoideus muscle; however, the needle was inserted more deeply and at a location medial to the insertion of the first electrode (Fig. 2B). A third, monofilar, insulated silver wire (HML, California Fine Wire Company) was stripped of insulation for the first 0.5 mm of the lead and was similarly implanted under the skin on the bird's dorsal surface above the vertebral column and served as a ground electrode. The bipolar electrodes inserted into the pectoralis and supracoracoideus were fed cranially and dorsally over the left shoulder joint and then caudally along the back, running near the point of insertion of the ground electrode. All three wires were then sutured together on the intervertebral fascia on the dorsal side of the animal. Fig. 2 illustrates the approximate location of placement of each of the two bipolar recording electrodes. Once the surgery was complete the anaesthesia was withdrawn and the birds were allowed to recover. Recovery was considered complete when birds were readily able to sustain hover feeding.

Experimental design

The experiment was conducted in a testing arena that was 61×62×76 cm (width×length×height). Beginning several days prior

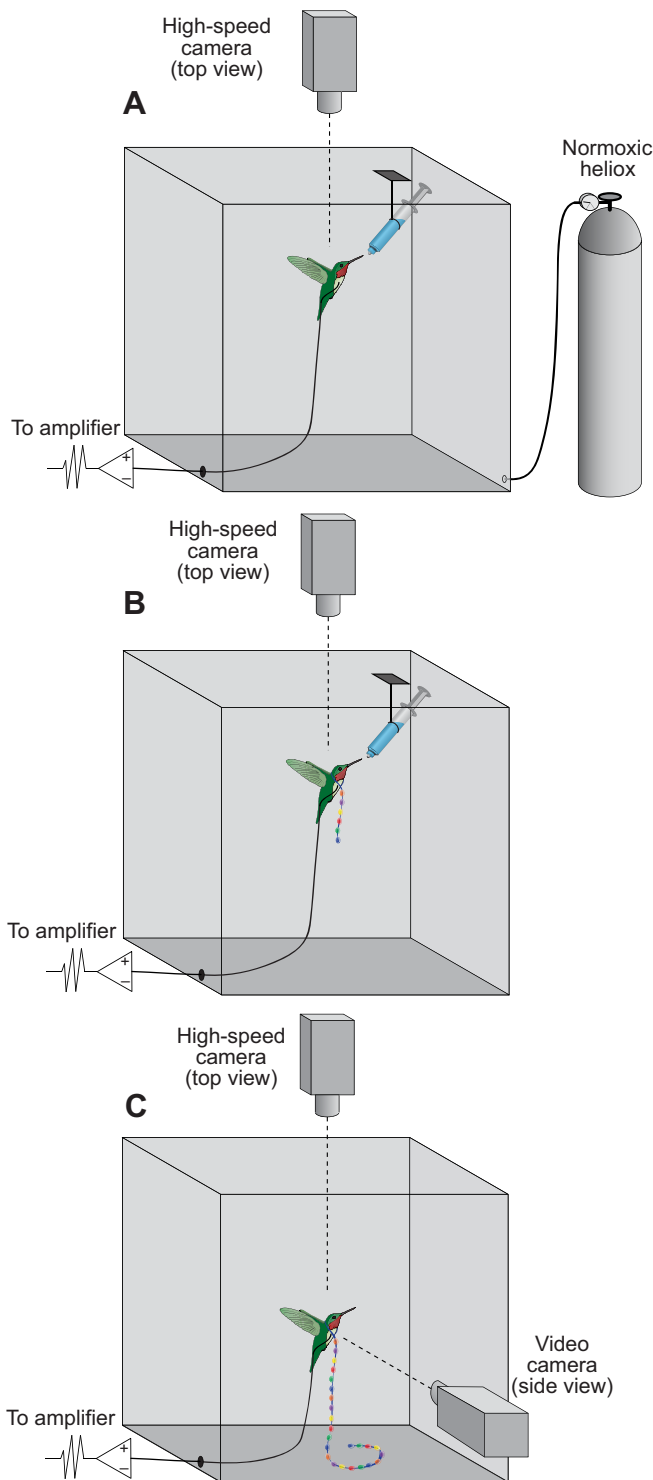


Fig. 1. Experimental set-up for *in vivo* recordings under multiple hovering challenges. (A) Air density reduction trials and unweighted hovering in normodense air were examined while a hummingbird fed from a suspended feeder. A high-speed video camera recorded wingbeat kinematics from an overhead view. Bipolar electrodes were inserted into the left pectoralis and supracoracoideus of the bird. For the hypodense condition, air density was decreased by progressive replacement of ambient air in the air-tight chamber with heliox. Unweighted hovering trials were conducted using an identical set-up except that no heliox replacement was attempted. (B) Sub-maximal load-lifting trials were performed as each bird hover fed in normodense air while lifting a 0.25, 0.5 or 0.75 g string of beads placed around its neck. (C) Maximal load-lifting performance in normodense air was assessed as each bird was placed at the bottom of the arena with a string of colour-coded beads fixed around its neck *via* a harness. The birds flew upwards until the weight of the beads lifted off the floor equalled the maximum load they could briefly bear while transiently hovering.

al., 2010b), (2) hovering at a feeder in progressively less dense normoxic (heliox-ambient) air mixtures (Chai and Dudley, 1996; Altshuler et al., 2010b), (3) hovering at a feeder while lifting progressively heavier sub-maximal loads (Wells, 1993), and (4) hovering briefly while lifting maximal loads (Fig. 1) (Chai et al., 1997; Altshuler et al., 2004; Altshuler et al., 2010a; Altshuler et al., 2010b).

Air density was reduced in the air-tight test arena by progressive replacement of normal air at Scarborough, ON, Canada (elevation 76 m, density 1.178 kg m^{-3}) with normoxic heliox (21% oxygen, balance helium; density 0.41 kg m^{-3}) at a rate of 8.51 min^{-1} . Air density was calculated following measurement of barometric pressure, temperature and humidity. Following each hover-feeding event, a Galton whistle was blown inside the arena and fundamental changes in frequency were used to calculate the reduced air density, relative to normodense air (see Altshuler et al., 2010b). Through trial and error we were able to time hover-feeding events to coincide with air density values of $\sim 1, 0.9, 0.8$ and 0.7 kg m^{-3} . Birds consistently failed to sustain hovering at the artificial feeder at densities lower than 0.7 kg m^{-3} .

Following air density reduction feeding trials, the door to the chamber was opened and the density inside the chamber was allowed to return to normal. Then, after recording data during at least one subsequent feeding while the birds were hovering in normal air, birds were subjected to a series of load-lifting trials. Submaximal loads consisting of a short string of beads connected to a rubber harness were applied to birds by placing the harness around an individual's neck. Loads with total masses of 0.25, 0.5 or 0.75 g were constructed prior to data collection. Birds were accustomed to perching and hover feeding while wearing loads during training periods prior to data collection (see above). Recordings were collected of birds hover feeding while lifting each submaximal load in a randomized order. Recordings were discarded from analysis when any individual was not able to fly from the perch, feed for a minimum of 2 s, and fly back to the perch successfully, as failure to do so was taken as an indication that the bird could not sustain the load.

Following all submaximal load-lifting trials, the harness was removed and the bird was allowed to recover for a minimum of 20 min. Then, data were recorded while the unloaded bird hover fed in normodense air. Following this baseline trial, birds were subjected to maximum load-lifting trials. The attachment of weight *via* a harness placed around the neck was identical to that employed during submaximal load lifting except that the chain was significantly

to data collection, the birds were trained to perch, fly and feed, both unweighted and while wearing small weights (see below). A 1 ml disposable syringe served as the artificial feeder. Birds were trained to hover feed on command by occluding the feeder opening with a small shield and allowing access for only brief durations at regular intervals every 10–20 min. Muscle activation and wingbeat kinematics were studied for all four birds under the following conditions: (1) hovering at a feeder (in ambient air without any load attached) (Chai and Dudley, 1996; Chai et al., 1997; Altshuler et

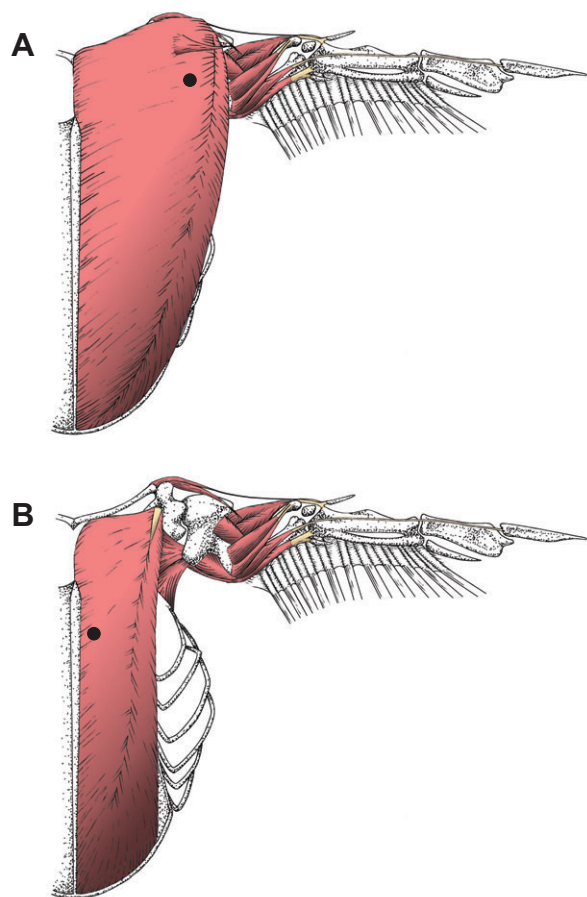


Fig. 2. An illustration of the musculoskeletal anatomy of small hummingbirds (modified from Welch and Altshuler, 2009). Markings indicate the position of electrode placement in (A) the pectoralis and (B) the supracoracoideus muscle. Note the illustration in B is identical to that in A except that the pectoralis has been removed to show the supracoracoideus muscle, which lies beneath it.

longer and included beads of known individual mass, spaced at ~1 cm intervals, weighing collectively more than the hummingbird could lift. Birds were released from the floor of the arena and promptly flew directly upwards, as is their natural escape response, lifting progressively greater weight, until reaching a maximum elevation and load. Birds transiently hovered while lifting this maximal load before descending. A minimum of three maximal load-lifting trials were recorded, until we were satisfied that maximum flight effort had been elicited. A camera captured video from a side view, which allowed us to determine the number of beads, and thus maximum mass, lifted. The trial that resulted in the bird lifting the maximum number of beads was chosen for further analysis. A recording of unweighted hover feeding in normodense air was obtained following the maximal load-lifting trial. The electrodes were then removed from the bird under anaesthesia.

Electromyography

During each trial listed above, the electrode wires coming from the bird remained connected to cable leads near the bottom edge of the arena. Sufficient electrode lengths were employed such that the leads remained slack at all times, and the lifted length never exceeded ~70 cm. EMG signals were amplified 1000 \times with an extracellular amplifier (A-M Systems, differential AC amplifier, model 1700,

Sequim, WA, USA). Amplifier filters were set to low and high frequency cut-offs of 0.1 Hz and 10 kHz, respectively. The analog signals were acquired using an analog-to-digital converter (Digidata 1440A, Molecular Devices, Sunnyvale, CA, USA) sampling at 10 kHz. EMG signals were recorded to PC using Axoscope (v.10.3, Molecular Devices) and were synchronized with high-speed video recordings *via* two mechanisms (see below). The transistor–transistor logic (TTL) signal that triggered the end of video recording was acquired on an additional channel of the amplifier. An additional analog-to-digital converter (National Instruments, Vaudreuil-Dorion, QC, Canada) was also used, and both EMG (including the trigger) and videographic data were simultaneously recorded to PC using MIDAS DA (Xcitex, Cambridge, MA, USA). This latter analog-to-digital converter was not as precise because it recorded at a maximum frequency of 1000 Hz. However, it provided an independent means of confirming synchronization of the EMG and video data. To facilitate statistical analysis and comparisons among individuals and among muscles, the EMG signals were post-processed. A zero-phase, fourth-order high-pass Butterworth filter with a cut-off frequency set at ~12 times the wingbeat frequency was used to remove movement artifacts and set the mean of the inactive portions of the signal to zero. EMG area (the rectified area of each EMG burst), EMG amplitude (the height of each spike within each burst), EMG onset (the start of EMG activity prior to the beginning of the downstroke for the pectoralis and the start of EMG activity prior to the beginning of the upstroke for the supracoracoideus) and number of spikes per burst were calculated as previously (Altshuler et al., 2010b). The spike threshold was set to 0.25 times the highest spike amplitude during each run, in order to automate the detection of discrete spikes and determine the number of spikes per burst. EMG spike amplitude and EMG area were each normalized against the maximum EMG spike amplitude or area, respectively, for each bird across all trials.

Kinematic analysis

All flight trials were filmed using a high-speed video camera (S-PRI, AOS Technologies AG, Baden Daettwil, Switzerland), which recorded at 1000 frames⁻¹ at a shutter speed of 250 μ s. The camera was located above the arena and recorded video from an overhead view. Wingbeat frequency was calculated by dividing the recording frequency by the number of frames necessary for completion of a full wingbeat. Stroke amplitude was calculated by deriving the angular distance covered by each wing from the top of the upstroke (wrist pronation) to the bottom of the downstroke (wrist supination) rotating about each shoulder. At each of these extreme positions, the wings appeared as thin lines when viewed from above. The same 15 consecutive wingbeats were analysed for both wingbeat kinematics and EMG characteristics. Only wingbeats that occurred when the bird was stationary at the feeder, or relatively stationary and at a maximum elevation during asymptotic load-lifting trials, were analysed. Angular velocity was calculated by dividing stroke amplitude (in radians) by the time taken to complete a half stroke.

Morphological measurements

The mass of each bird was measured at the beginning and end of each experiment using a digital balance with a precision of 0.1 mg (MS-104S, Mettler Toledo, Mississauga, ON, Canada). The mean of the two measurements constituted the estimated mass of the bird during all trials.

Statistical analysis

All kinematic and EMG variables were averaged across the 15 analysed wingbeats for each bird within each treatment. Data were

analysed using repeated measures ANOVA using the statistical program SPSS (v.17.0, IBM) to test for statistically significant differences among treatment means in EMG and kinematic parameters as a function of treatment level. Muscle type was included as a factor to test for differences in EMG parameters between the supracoracoideus and pectoralis. Because birds were similar in mass, and because the maximum loads each bird lifted were also quite similar (1.92 ± 0.14 g), values of mass lifted were binned at average values of 2.8, 3.05, 3.3, 3.55 and 4.72 g (for maximum load lifting). If the data violated the test of sphericity, the Greenhouse–Geisser, Huynh–Feldt and lower bound correction factors were applied to adjust the degrees of freedom and significance values. Lower bound corrected values are reported because the lower bound correction is the most conservative of the three. A mixed-effects non-linear model incorporating individual as a random factor was fitted using the lme4 package (v.0.999999-2) in the statistical program R (v.2.15.3) in order to examine whether experiment type, load lifting *versus* air density reduction, was a significant factor influencing the relationship between neuromuscular activation intensity (EMG area) and angular velocity of the wing tip. The results were considered significant if P -values were less than 0.05. Data are presented below as the mean \pm s.d. of values of the four birds.

RESULTS

Regulation of wingbeat kinematics *via* neural input across varying aerodynamic power output requirements

Wingbeat kinematics as a function of either total mass lifted or air density are shown in Fig. 3. Within air density reduction trials, stroke amplitude increased significantly from 140.9 ± 11.2 deg in ambient air to 160.9 ± 6.8 deg in the lowest air density ($F_{4,12}=17.47$, $P<0.03$; Fig. 3A); however, stroke amplitude never reached values as high as those observed during maximal load-lifting assays (see

below). Wingbeat frequency increased significantly as a function of declining air density ($F_{4,12}=4.55$, $P=0.02$; Fig. 3B). However, this trend was driven by the value at the lowest air density (58 ± 3 Hz at 0.7 kg m^{-3}) and wingbeat frequency did not vary significantly as a function of air density when the lowest air density trials were excluded (54 ± 2 to 56 ± 2 Hz between 1.2 and 0.8 kg m^{-3} ; $F_{3,9}=1.29$, $P=0.34$). Stroke amplitude increased significantly as the birds hover fed while lifting progressively heavier loads, ranging from 140.9 ± 11.2 deg when birds were unloaded (2.8 g total) to 157.3 ± 10.8 deg while lifting a total of 3.55 g ($F_{1,3}=24.35$, $P=0.02$; Fig. 3C). During maximal load-lifting trials ($68.22 \pm 5.43\%$ of body mass was briefly lifted), stroke amplitude reached an average of 174.3 ± 5.1 deg, which is close to the geometrical constraint of ~ 180 deg (Fig. 3C). Wingbeat frequency did not vary significantly among sub-maximal load-lifting trials, ranging from 54 ± 3 to 57 ± 2 Hz ($F_{3,9}=1.29$, $P=0.34$; Fig. 3D). Wingbeat frequency was 57 ± 2 Hz during maximal load lifting, which was not significantly greater than the wingbeat frequencies exhibited during sub-maximal load lifting ($F_{4,12}=1.26$, $P=0.34$; Fig. 3D).

As a first step in analysing EMG data, the hovering trials that were conducted in normodense air at the beginning of the experiment and between the different flight challenges were compared. We found no significant differences in wingbeat kinematics or EMG waveforms (see below) from either the pectoralis or supracoracoideus across each of the unweighted hover feedings in normodense air (data not shown). This confirmed electrode placement did not change throughout the trial period.

Sample EMG traces from the pectoralis and supracoracoideus shown in Fig. 4 are direct outputs from the amplifier with analog filter cut-offs of 1 Hz and 10 kHz, prior to any post-processing. EMG traces from the pectoralis and the supracoracoideus muscles of ruby-throated hummingbirds are composed of a discrete number of spikes per burst during hovering flight under both load-lifting trials and

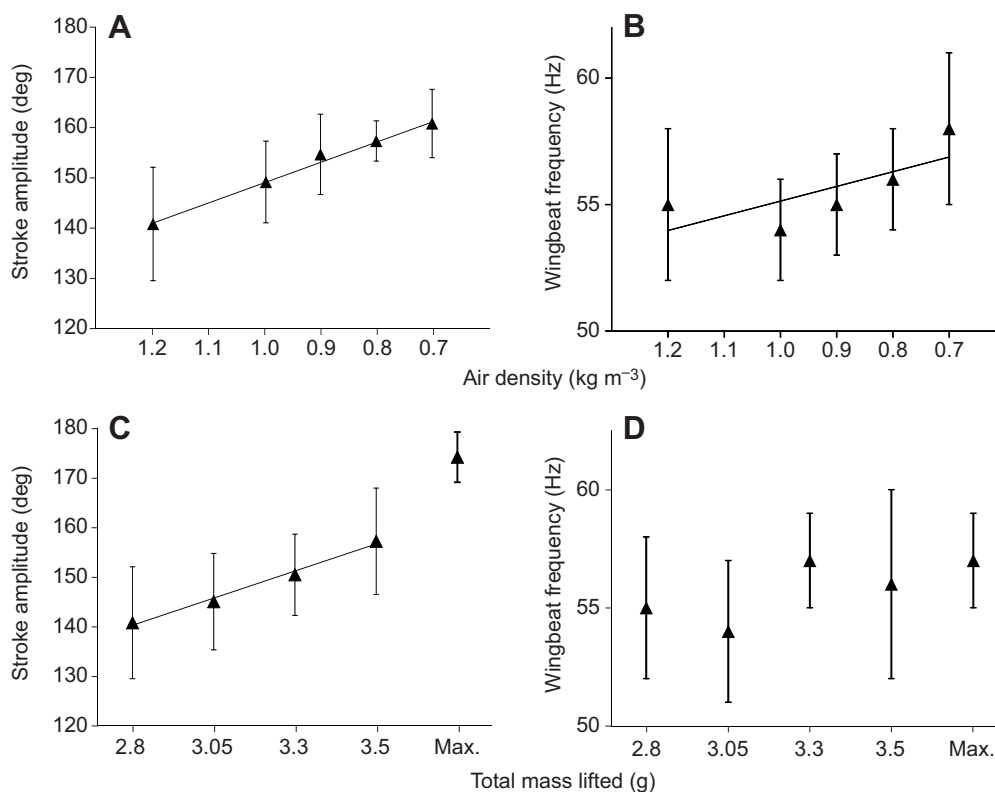


Fig. 3. Wingbeat kinematics [stroke amplitude (A,C) and wingbeat frequency (B,D)] in relation to experimental treatments [air density (A,B) or total mass lifted (C,D)] for hovering ruby-throated hummingbirds (*Archilochus colubris*). Data are binned according to treatment level. Symbols represent the mean (\pm s.d.) of $N=4$ individuals. Trend lines are for illustration only and are included only when variation in the data across treatment means was significant.

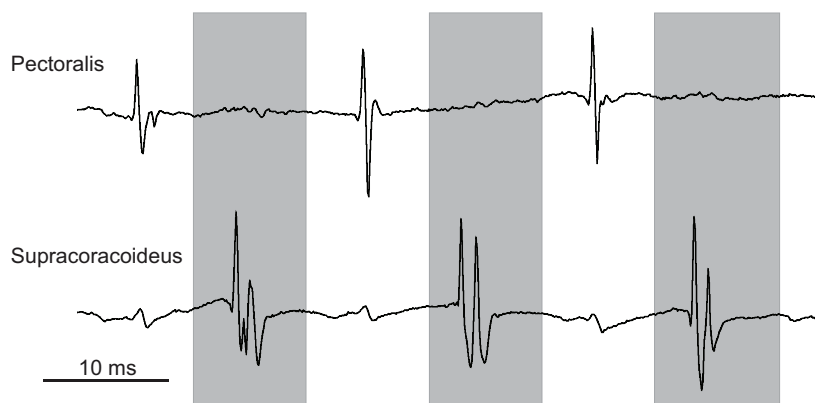


Fig. 4. Sample electromyographic (EMG) recordings of both flight muscles while the bird was hovering in ambient air lifting 0.75 g in excess of body mass. Using detection criteria defined in Materials and methods, exactly 1 spike per burst in the pectoralis and 2 spikes per burst in the supracoracoideus were counted in each of the bursts shown. Note: signals are direct outputs from the amplifier with analog filter cut-offs of 1 Hz and 10 kHz, prior to any post-processing. Shaded areas correspond to the downstroke of the wing.

air density reduction trials. Whenever the hummingbirds sustained hovering at the feeder, regardless of the flight challenge, the number of spikes per burst averaged 1–2 (see Fig. 5A,C). However, this increased to 2.5–3 spikes per burst during maximal load-lifting assays. Across air density reduction trials the number of spikes did not increase significantly; the pectoralis exhibited an average of 1.35 ± 0.23 spikes per burst ($F_{4,12}=2.82$, $P=0.07$), whereas the supracoracoideus exhibited 1.90 ± 0.36 spikes per burst ($F_{4,12}=27.874$, $P=0.67$; Fig. 5A). Across all sub-maximal load-lifting trials the number of spikes per burst did not increase significantly; the pectoralis exhibited an average of 1.32 ± 0.28 spikes per burst ($F_{1,3}=1.27$, $P=0.34$) and the supracoracoideus exhibited 1.78 ± 0.32 spikes per burst ($F_{1,3}=2.43$, $P=0.22$; Fig. 5C). Compared with the mean values across submaximal load-lifting trials, the number of spikes per burst increased significantly during maximal asymptotic load-lifting trials; the pectoralis exhibited 2.57 ± 0.38 spikes per burst ($F_{4,12}=22.39$, $P<0.001$) and the supracoracoideus exhibited 2.8 ± 0.59 spikes per burst on average ($F_{4,12}=5.78$, $P=0.008$).

Normalized EMG area (EMG area) increased significantly for the pectoralis from 0.30 ± 0.04 to 0.58 ± 0.02 ($F_{4,12}=5.92$, $P=0.007$) and for the supracoracoideus muscle from 0.31 ± 0.11 to 0.51 ± 0.10 ($F_{4,12}=5.81$, $P=0.008$) under air density reduction trials (Fig. 5B). EMG area of both flight muscles increased significantly across submaximal load-lifting assays and further during maximum load lifting (Fig. 5D). EMG area in the pectoralis increased significantly from 0.30 ± 0.04 to 0.86 ± 0.07 ($F_{1,3}=46.17$, $P=0.007$) as birds lifted 2.81 ± 0.09 g to the maximum load. EMG area also increased for the supracoracoideus from 0.31 ± 0.11 to 0.85 ± 0.05 as more mass was lifted ($F_{1,3}=75.50$, $P=0.003$). Some studies have used normalized EMG amplitude instead of normalized EMG area as a measure of the number of active motor units, but analysis of normalized EMG amplitude of the largest peak within a burst did not vary significantly when birds were lifting heavier loads or hovering in reduced air densities.

The activation of antagonistic muscles was completely out of phase with one another, with very little variation in timing relative to the wing stroke transition. Both the pectoralis and supracoracoideus muscles were activated and deactivated prior to the start of muscle

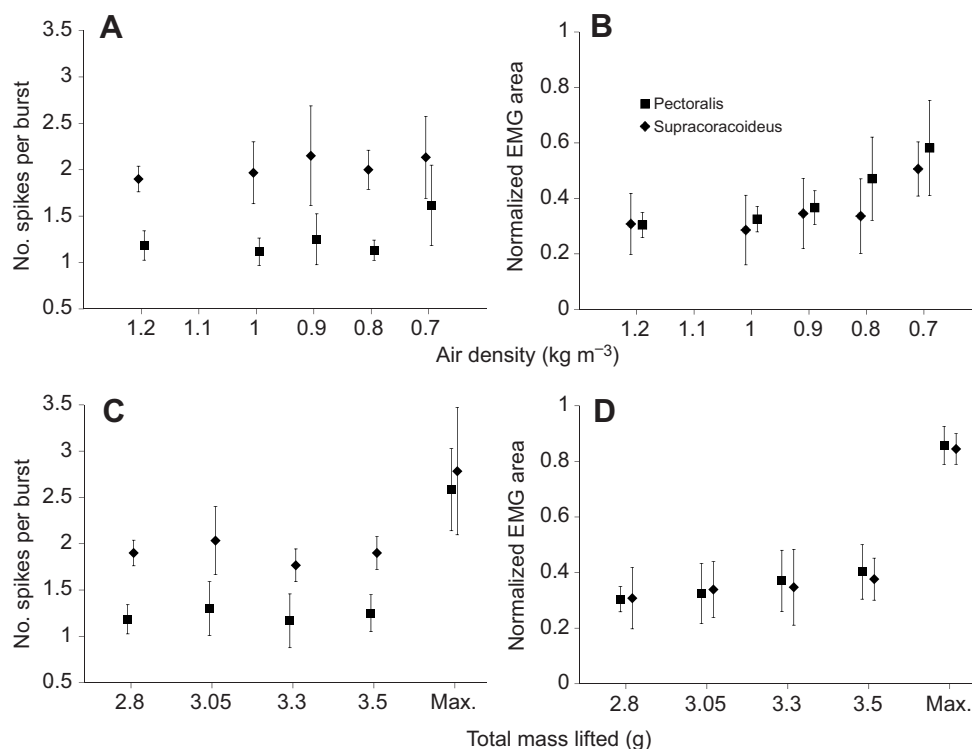


Fig. 5. Number of spikes per EMG burst (A,C) and normalized area of EMG bursts (B,D) in the pectoralis and supracoracoideus in relation to experimental treatment [air density (A,B) or total mass lifted (C,D)] for hovering ruby-throated hummingbirds. Data are binned according to treatment level. Values for the pectoralis and supracoracoideus are offset slightly for clarity. EMG area is normalized within individuals to the maximum value recorded across all trials. A threshold value of 0.25 of the maximum spike intensity within an individual trial (hovering at a given air density or with a given mass lifted) was applied to automate the detection of individual spikes within bursts. Symbols represent the mean (\pm s.d.) of $N=4$ individuals.

shortening (as indicated by wing movement). The timing of activation of the pectoralis muscle did not vary significantly across air density reduction trials, occurring on average 4 ms prior to the start of the downstroke ($F_{4,12}=0.31$, $P=0.87$; Fig. 6A). The timing of activation of the supracoracoideus muscle was also constant, occurring on average 5 ms prior to the start of the upstroke ($F_{4,12}=0.69$, $P=0.61$; Fig. 6A). Though the number of spikes per burst did not vary, EMG duration (measured from the start of the first spike to the end of the final spike in the burst) increased significantly as air density decreased in both the pectoralis ($F_{4,12}=15.23$, $P<0.0001$) and the supracoracoideus ($F_{4,12}=29.42$, $P<0.0001$; Fig. 6C). EMG duration in the pectoralis ranged from 1.45 ms to a maximum of 2.97 ms across air densities (7.48% to 18.27% of the wingbeat). The supracoracoideus EMG duration ranged from 1.72 to 4.22 ms (8.79% to 25.71% of the wingbeat). The timing of activation of the pectoralis muscle prior to the downstroke did not vary significantly among load-lifting trials, occurring 4 ms prior to the start of the downstroke ($F_{4,12}=1.00$, $P=0.45$; Fig. 6B). Similarly, the onset of EMGs of the supracoracoideus prior to the upstroke did not vary among load-lifting trials, occurring 5 ms prior to the start of the upstroke ($F_{4,12}=2.05$, $P=0.15$; Fig. 6B). EMG duration also increased significantly as the birds lifted greater loads for both the pectoralis ($F_{4,12}=28.67$, $P<0.0001$) and the supracoracoideus ($F_{4,12}=29.42$, $P<0.0001$; Fig. 6D). Under load-lifting trials the EMG duration of the pectoralis and supracoracoideus ranged from 1.49 to 4.61 ms (7.64% to 24.76% of the wingbeat) and 1.72 to 5.35 ms (8.79% to 28.55% of the wingbeat), respectively.

Comparing the activation patterns of the supracoracoideus and the pectoralis

The difference between the mean values of all four EMG parameters of the pectoralis and supracoracoideus followed the same patterns within both air density reduction and load-lifting trials. On average, normalized EMG area did not significantly differ between the two muscles across air density reduction trials (Fig. 5B) ($F_{1,6}=0.770$, $P=0.414$) or among load-lifting trials (Fig. 5D) ($F_{1,6}=0.025$, $P=0.88$).

Hence, the intensity of activation of motor units, relative to the maximal activation observed at any point during the trials, did not differ between the two primary flight muscles.

The number of spikes per burst was significantly greater in the supracoracoideus than in the pectoralis within both air density trials and load-lifting trials. Across all the air density reduction trials the supracoracoideus exhibited 0.77 ± 0.26 more spikes per burst (1.61 times as many spikes per burst) than the pectoralis (Fig. 5A) ($F_{1,6}=27.874$, $P=0.002$). Across all sub-maximal load-lifting trials the supracoracoideus exhibited 0.68 ± 0.27 more spikes per burst (1.55 times as many spikes per burst) than the pectoralis (Fig. 5C) ($F_{1,6}=20.52$, $P=0.004$). During maximal load lifting the supracoracoideus exhibited 0.23 ± 0.60 more spikes per burst (1.08 times as many spikes per burst) than the pectoralis ($F_{1,6}=14.36$, $P=0.009$; Fig. 5C).

EMG onset was significantly earlier in the supracoracoideus than in the pectoralis, measured with respect to the relevant wingbeat transition. During air density reduction trials, the supracoracoideus was activated 1 ms earlier ($6.22\pm1.22\%$ earlier in the wingbeat), relative to the subsequent wingbeat transition, than the pectoralis ($F_{1,6}=5.83$, $P=0.044$; Fig. 6A). During load-lifting trials, the supracoracoideus was activated 1 ms earlier ($4.18\pm0.77\%$ earlier in the wingbeat), relative to the subsequent wingbeat transition, than the pectoralis ($F_{1,6}=4.42$, $P=0.035$; Fig. 6B).

The EMG duration was significantly longer in the supracoracoideus than in the pectoralis. On average, during air density reduction trials, the supracoracoideus was activated 0.80 ± 0.33 ms longer than the pectoralis ($F_{1,6}=10.96$, $P=0.016$; Fig. 6C). During load-lifting trials, the supracoracoideus was activated, on average, 0.72 ± 0.20 ms longer than the pectoralis ($F_{1,6}=15.86$, $P=0.007$; Fig. 6D).

Influence of air density on the relationship between muscle activation and wingbeat kinematics

Previous research in birds has demonstrated that normalized EMG area is a strongly correlated with peak muscle force, strain rate and

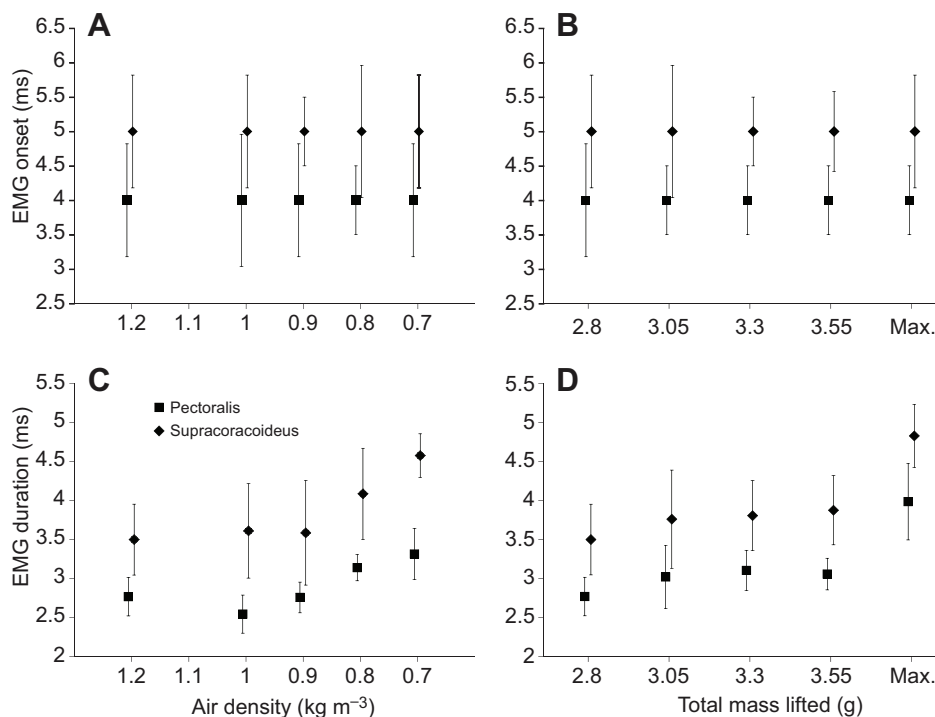


Fig. 6. Timing (onset of EMG activity prior to ensuing wingtip reversal; A,B) and duration of the EMG burst (C,D) in the pectoralis and supracoracoideus in relation to experimental treatments [air density (A,C) or total mass lifted (B,D)] for hovering ruby-throated hummingbirds. Data are binned according to treatment level. Values for the pectoralis and supracoracoideus are offset slightly for clarity. Symbols represent the mean (\pm s.d.) of $N=4$ individuals.

thus pectoralis power output during flight (Hedrick et al., 2003; Tobalske et al., 1997; Ellerby and Askew, 2007). Data presented here strongly suggest that as hovering power output requirements increase (with either decreasing air density or increasing load), flight muscle EMG area also increases. In order to understand whether air density influenced the translation of muscle activation into wingbeat kinematics, we constructed a model that related EMG area, trial type and the interaction of these two parameters to the mean angular velocity of the wingtip. Individual was included as a random factor in the model design and models were fitted to the pectoralis and supracoracoideus separately. Using the languageR package (v.1.4) in the R statistical programming environment, we estimated confidence intervals and *P*-values for model parameters. As shown in Table 1, EMG area of the pectoralis or supracoracoideus was the only significant predictor of mean angular velocity of the wingtip in each model (pectoralis: *P*<0.0001; supracoracoideus: *P*<0.0001). Neither the experiment type nor the interaction between experiment type and EMG area was a significant predictor (*P*>0.2 in all cases; see Table 1).

DISCUSSION

Ruby-throated hummingbirds increased performance during sustained hovering (in air density reduction and submaximal load-lifting trials) primarily through increases in wing stroke amplitude while increases in wingbeat frequency were only observed when hovering at the lowest air density. Surprisingly, we did not observe significant increases in wingbeat frequency during maximal load-lifting assays. While data from the lowest air density trial appear to be driving the trend in wingbeat frequency in our data, Chai and Dudley have previously reported a consistent increase in wingbeat frequency in ruby-throated hummingbirds subjected to progressive heliox replacement (Chai and Dudley, 1995; Chai and Dudley, 1996). Thus, we feel confident that the trend we observed reflects a biologically relevant pattern. The differences in reliance on stroke amplitude and/or wingbeat frequency increase to generate more power output dependent on the nature of the flight challenge are consistent with findings from studies on a variety of small hummingbird species (Wells, 1993; Chai and Dudley, 1995; Chai and Dudley, 1996; Altshuler and Dudley, 2003; Altshuler et al., 2004; Altshuler et al., 2010a). However, this is the first study to report such variation in kinematic adjustments and the first to investigate flight muscle EMG patterning in individual hummingbirds subjected to asymptotic load lifting and multiple distinct challenges to sustained hovering flight.

Ruby-throated hummingbirds activate each of the two major flight muscles with one to three simultaneous bursts of motoneuron action potentials, eliciting muscle fibre action potentials in the pectoralis and supracoracoideus, prior to the corresponding wing stroke. The

number of spikes per EMG burst is similar to that seen in other hummingbirds, and is substantially lower than that observed in other avian taxa (Hagiwara et al., 1968; Altshuler et al., 2010b; Tobalske et al., 2010; Hedrick et al., 2003; Ellerby and Askew, 2007; Tobalske and Dial, 1994). The increases in stroke amplitude observed during sustained hovering in hypodense air or while lifting submaximal loads was associated with increases in EMG burst intensity (area) but not with changes in spike number per burst. The data presented here and in the studies mentioned above imply consistency in the neuromuscular and kinematic approaches to varying power output that small hummingbirds employ during sustainable hovering or forward flight (Chai and Dudley, 1995; Chai and Dudley, 1996; Wells, 1993; Altshuler et al., 2010b; Tobalske et al., 2007; Tobalske et al., 2010). In contrast to sustained hovering, both EMG area and spike number per burst increased substantially in both the pectoralis and supracoracoideus in order to generate significantly greater stroke amplitudes and angular velocities during maximal load lifting, a pattern also seen in the pectoralis of Anna’s hummingbirds (Altshuler et al., 2010b). Overall, these data suggest that ruby-throated hummingbirds employ spatial recruitment of motor units to drive sustainable increases in stroke amplitude while both spatial and temporal recruitment of motor units is required to achieve the greatest stroke amplitudes at high wingbeat frequencies during burst hovering in both major flight muscles, a finding consistent with previous reports (Altshuler et al., 2010b; Tobalske et al., 2010).

Steady hover feeding in hypodense heliox gas mixtures and while lifting submaximal loads is an exclusively or predominantly aerobically powered activity, given it can be sustained for more than several seconds and as evidenced by the simultaneous rise in estimated mechanical power output and oxygen consumption rate, and resulting invariant muscle efficiency (Chai and Dudley, 1996; Wells, 1993). In contrast, we assume asymptotic maximal load lifting is dependent on supplemental anaerobic metabolic power input because hummingbirds cannot sustain maximal hovering effort for more than ~1 s and subsequently pant heavily for a few moments after descending to the chamber floor. The distinctive EMG waveform patterns associated with differences in the sustainability of muscle performance are striking. Our data show that a given proportion of motor units are activated on average once per wingbeat in the pectoralis and once or twice per wingbeat in the supracoracoideus with each wingbeat at frequencies of ~55–60 Hz, and suggest that activation of fibres at this frequency is entirely aerobically powered. In contrast, the activation of a greater proportion of motor units, potentially 2–3 times per wingbeat, during maximal hovering appears to surpass an aerobically sustainable threshold.

Evidence from sonomicrometry in the pectoralis in combination with high-speed recordings and analysis of wingbeat kinematics

Table 1. Mixed effects regression model of the relationship between mean angular velocity of the wingtip during hovering, the intensity of muscle activation (normalized EMG area) and the experiment type (air density reduction or load lifting)

Muscle	Parameter	Mean angular velocity of the wingtip	
		95% CI estimate	<i>P</i>
Pectoralis	EMG area	(60.58, 117.04)	<0.0001*
	Experiment type	(−26.34, 61.05)	0.4133
	EMG area × experiment type	(−184.29, 47.21)	0.2358
Supracoracoideus	EMG area	(59.97, 216.39)	<0.0001*
	Experiment type	(−34.36, 46.86)	0.9231
	EMG area × experiment type	(−167.14, 59.70)	0.4471

Note: individual is included as a random effect.
CI, confidence interval.

suggests that the wings are 'kinematically rigid' and that wingtip position is an accurate proxy of flight muscle strain (Tobalske et al., 2007). In ruby-throated hummingbirds, flight muscle activation begins about halfway into the prior half-stroke, when each muscle is lengthening. In addition, we found EMG activity ceased in each flight muscle before the start of the subsequent half-wingbeat, and thus before muscle shortening, across all hovering behaviours examined, consistent with findings in Anna's and rufous hummingbirds (Altshuler et al., 2010b; Tobalske et al., 2010). Because the wingbeat frequencies in each species were all greater than 40 Hz (Altshuler et al., 2010b; Tobalske et al., 2010) it seems possible that the cessation of EMG activity prior to muscle shortening is a general feature of flight muscles operating near or above this frequency. Burst durations increased as mechanical power output requirements increased and were longest during maximal load-lifting assays. Because burst duration calculated as the length of time that the rectified EMG signal was different from 0 V, the significant increase in burst duration across sustained challenges while spike number remained constant is likely to be simply a reflection of the overall greater area (i.e. 'height' × 'width') of these individual EMG spikes. Importantly, the significant increase in burst duration and spike number seen during maximal load lifting means the flight muscles maintain tension later into the wingbeat cycle. As wingbeat frequency either stays the same or increases during maximal load lifting compared with sustained hovering in normodense air, this implies that the shorter EMG burst duration and synchrony of fibre activation observed during sustained hovering are not solely the consequence of a constrained activation window that would allow sufficient time for relaxation to occur. Rather, it is the maximal burst durations observed during brief load lifting that may be constrained within the maximum allowable activation window.

While stroke amplitude increased both as a function of lower air density and while birds sustainably lifted progressively more mass, wingbeat frequency also increased at low air densities. These findings confirm that interspecific variation in hovering flight behaviour does not, by itself, explain the differences in kinematics observed between flight challenge types previously (Wells, 1993; Chai and Dudley, 1995; Chai and Dudley, 1996; Altshuler et al., 2010b). Further analysis is required to determine whether the differences in kinematics observed with each trial type are the result of active variation in neural programming, or the consequence of differences in drag imposed on the wing by variation in air density in one trial type, but not the other. Aerodynamic theory predicts that profile drag, which accounts for a significant portion of total calculated aerodynamic power requirements in hovering hummingbirds (Wells, 1993; Altshuler, 2001), decreases as air density declines. Thus, it is possible that for a given neuromuscular input, and resulting muscle force, lower profile drag may result in greater wing acceleration in hypodense air. We examined the effect of neural input on resulting wing acceleration by fitting a model with normalized EMG area, experiment type and their interaction term as factors. Mean angular velocity of the wingtip was chosen as the dependent variable because this kinematic parameter captures variation in both stroke amplitude and the duration of the wingbeat. Individual was included as a random factor. As shown in Table 1, only EMG area was found to be a significant predictor of variation in mean angular velocity of the wingtip. The fact that neither experiment type nor the interaction term was found to be a significant predictor indicates that the relationship between neuromuscular input (i.e. relative intensity of muscle activation) and mean angular velocity is consistent regardless of air density. It is

possible that other wingbeat parameters, such as attack angle, vary with air density in a way that offsets the decline in drag on the wing. However, assuming this is not the case, we hypothesize that while the wing may be accelerated more easily through hypodense air, achieving a comparatively greater mean angular velocity, each flight muscle must provide additional power to decelerate the wing in advance of the stroke transition.

We observed a slight trend towards increased wingbeat frequency during maximal load lifting compared with unweighted hovering in normodense air. However, in contrast to previous findings (Chai et al., 1997), this increase was not significant. Wingbeat frequencies of ruby-throated hummingbirds during hovering flight in normodense air were between 51 and 57 Hz, and frequencies during maximally loaded flight were between 54 and 58 Hz. Chai et al. reported frequencies of 49–52 Hz for hovering flight in normodense air and frequencies of 57–58 Hz for maximally loaded ruby-throated hummingbirds (Chai et al., 1997). Although the range in the values between our two studies is comparable, the wingbeat frequencies observed in our birds during unweighted hovering in normodense air were slightly higher than those in the previous study (Chai et al., 1997). It is unclear whether this discrepancy is due to anything more than sampling error or interindividual variation. However, it should be noted that the birds studied by Chai and colleagues (Chai et al., 1997) were not implanted with electrodes. It is possible that implantation of the electrodes in our birds may have affected kinematic performance. A study by Ellerby and Askew (Ellerby and Askew, 2007) found that implanting both EMG electrodes and sonomicrometry transducers in zebra finches and budgerigars results in significant differences in wingbeat kinematics. Because of time constraints, it was not possible for us to obtain a full set of control data in birds prior to electrode implantation. Still, in contrast to our findings, Anna's hummingbirds that were instrumented with electrodes did increase wingbeat frequency during maximal load-lifting assays (Altshuler et al., 2010b). Anna's hummingbirds are about 1.5 times larger than ruby-throated hummingbirds and exhibit a lower and broader range of wingbeat frequencies than those observed in ruby-throated hummingbirds in our study or that by Chai and colleagues (Chai et al., 1997). It is possible that electrode implantation also affected the wingbeat kinematics of hovering Anna's hummingbirds, though the effect was less pronounced. Unfortunately, data on the wingbeat kinematics of the individuals examined in the study by Altshuler et al. (Altshuler et al., 2010b), hovering while not implanted with electrodes, are also unavailable.

In comparison to the pectoralis, the supracoracoideus consistently exhibited more spikes per burst and burst duration was longer during all sustainable hovering trials. In addition, during all hovering behaviour, including maximal load lifting, the supracoracoideus was activated earlier prior to muscle shortening. The pectoralis and the supracoracoideus are both composed exclusively of type IIa (fast twitch oxidative-glycolytic) fibres (Suarez, 1992; Welch and Altshuler, 2009). Thus, significant differences in EMG waveforms between the two muscles cannot be related to variation in motor unit complement type or the relative activation timing of one motor unit type relative to another. We hypothesize two major differences in muscle anatomy may at least partly underlie the observed variation in EMG patterning. First, while the homogeneous complement of fibres in each muscle produces similar force per unit fibre cross-sectional area (Reiser et al., 2013), the physiological cross-sectional area of the supracoracoideus is substantially smaller. Thus, if a similar proportion of fibres are activated in each muscle, the supracoracoideus will produce less overall power output than the pectoralis. Because the hovering wingbeat is relatively

symmetrical, it is possible that the power output requirements from each muscle are, unlike their sizes, also relatively similar. As shown in this study and elsewhere (Altshuler et al., 2010b; Tobalske et al., 2010), increases in the temporal recruitment of fibres within a given hummingbird flight muscle, reflected as increases in spike number per burst, correlate with increased power output. Therefore, it seems plausible that the longer EMG duration and greater spike number per burst in the supracoracoideus compared with the pectoralis reflects relatively greater temporal recruitment of motor units in response to greater power demands per unit muscle mass. The second anatomical difference may underlie the earlier activation, relative to muscle shortening, observed in the supracoracoideus. The muscle–tendon unit anatomy is distinctly different between the pectoralis and supracoracoideus. Though the supracoracoideus originates on the keel of the sternum, deep relative to the pectoralis, the distal tendon passes through the shoulder and inserts on the dorsal side of the humerus acting to elevate the wing (Zusi and Bentz, 1984). No long tendon attaches to the pectoralis at either its origin or insertion points. We hypothesize that neural activation occurs earlier in the supracoracoideus relative to muscle–tendon unit shortening because there is greater compliance of series elastic components (principally, this long tendon). Generally, the long, thin tendons attached to the belly of pennate distal hindlimb muscles of vertebrates with short fibres are highly compliant (Roberts, 2002). Muscles with tendons that are highly compliant expend a large fraction of their shortening capacity stretching the tendon rather than causing skeletal movements directly. If, as we hypothesize, there is greater elastic compliance in the wing elevator muscle (supracoracoideus) than in the depressor (pectoralis) of hummingbirds, then it follows that the contribution of elastic energy storage and recovery may play a relatively greater role in the deceleration and subsequent reacceleration of the wing during the downstroke-to-upstroke transition. Such asymmetry of elastic energy recovery in the otherwise relatively symmetrical hummingbird hovering wingbeat should be considered as the finer aspects of cumulative power output during hovering are investigated.

The neuromuscular encoding of the modulation of wingbeat kinematics during sustained hovering flight appears highly conserved across species and hovering flight challenges. Ruby-throated hummingbirds adopt subtly different kinematic solutions to adjust flight performance when lifting sustainable loads as opposed to when hovering in hypodense air. Despite the reduction in drag on the wing, high stroke amplitudes at moderately higher wingbeat frequencies while hovering in hypodense air necessitate comparable increases in flight muscle activation, presumably as higher forces are needed to decelerate the wings prior to stroke transition. The high wingbeat frequencies of ruby-throated hummingbirds limit the amount of time available for the activation and deactivation of primary flight muscles. The limited activation window has resulted in motor unit recruitment being highly synchronized. With a single fibre type present in both major flight muscles, and one or two spikes per burst during all sustained flight behaviours, it seems Anna's (Altshuler et al., 2010b), rufous (Tobalske et al., 2010) and ruby-throated hummingbirds (this study) all modulate power output at high operating frequencies largely or exclusively by varying spatial recruitment in each muscle. Nonetheless, the fact that hummingbirds can increase spike number and burst duration during maximal burst hovering suggests that constraints on burst duration during sustained hovering are aerobic, rather than mechanical. While these results confirm that the relatively symmetrical hummingbird wingbeat is achieved by relatively similar changes in the intensity of activation of the antagonist primary flight

muscles, variation in the timing of activation and number of spikes per EMG burst was consistently different between the two muscles, probably reflecting differences in muscle morphology and compliance.

ACKNOWLEDGEMENTS

Shanchai Zahid, Derrick Groom and Piravinthan Sithamparanathan assisted in collection of the data. We thank Douglas Altshuler for providing custom-authored MATLAB analysis tools, for guidance regarding data analysis, and for helpful discussion. We thank Mahinda Samarakoon for assistance with coding in R. We also thank two anonymous reviewers for their comments.

AUTHOR CONTRIBUTIONS

S.M. performed the experiments. Both authors jointly developed the experimental protocol, contributed to data analyses and interpretation, and prepared the manuscript.

COMPETING INTERESTS

No competing interests declared.

FUNDING

Funding for this research was provided by a Natural Sciences and Engineering Research Council of Canada (NSERC) Discovery Grant [no. 386466], a Canada Foundation for Innovation (CFI) Leaders Opportunity Fund grant [no. 25326], and an Ontario Research Fund, Research Infrastructure grant [no. 25326] to K.C.W.

REFERENCES

- Altshuler, D. L. (2001). Ecophysiology of hummingbird flight along elevational gradients: an integrated approach. PhD dissertation, University of Texas at Austin, Austin, TX, USA.
- Altshuler, D. L. and Dudley, R. (2003). Kinematics of hovering hummingbird flight along simulated and natural elevational gradients. *J. Exp. Biol.* **206**, 3139–3147.
- Altshuler, D. L., Dudley, R. and McGuire, J. A. (2004). Resolution of a paradox: hummingbird flight at high elevation does not come without a cost. *Proc. Natl. Acad. Sci. USA* **101**, 17731–17736.
- Altshuler, D. L., Dudley, R., Heredia, S. M. and McGuire, J. A. (2010a). Allometry of hummingbird lifting performance. *J. Exp. Biol.* **213**, 725–734.
- Altshuler, D. L., Welch, K. C., Jr, Cho, B. H., Welch, D. B., Lin, A. F., Dickson, W. B. and Dickinson, M. H. (2010b). Neuromuscular control of wingbeat kinematics in Anna's hummingbirds (*Calypte anna*). *J. Exp. Biol.* **213**, 2507–2514.
- Altshuler, D. L., Quicazán-Rubio, E. M., Segre, P. S. and Middleton, K. M. (2012). Wingbeat kinematics and motor control of yaw turns in Anna's hummingbirds (*Calypte anna*). *J. Exp. Biol.* **215**, 4070–4084.
- Chai, P. and Dudley, R. (1995). Limits to vertebrate locomotor energetic suggested by hummingbirds hovering in heliox. *Nature* **377**, 722–725.
- Chai, P. and Dudley, R. (1996). Limits to flight energetics of hummingbirds hovering in hypodense and hypoxic gas mixtures. *J. Exp. Biol.* **199**, 2285–2295.
- Chai, P., Chen, J. S. C. and Dudley, R. (1997). Transient hovering performance of hummingbirds under conditions of maximal loading. *J. Exp. Biol.* **200**, 921–929.
- Degernes, A. L. and Feduccia, A. (2001). Tenectomy of the supracoracoideus muscle to deflight pigeons (*Columba livia*) and cockatiels (*Nymphicus hollandicus*). *J. Avian Med. Surg.* **15**, 10–16.
- Ellerby, D. J. and Askew, G. N. (2007). Modulation of pectoralis muscle function in budgerigars *Melopsittacus undulatus* and zebra finches *Taeniopygia guttata* in response to changing flight speed. *J. Exp. Biol.* **210**, 3789–3797.
- Greenewalt, C. H. (1962). *Dimensional Relationships for Flying Animals*. Smithsonian Miscellaneous Collections Vol. 144, pp. 1–46. Washington, DC: Smithsonian Institution.
- Hagiwara, S., Chichibu, S. and Simpson, N. (1968). Neuromuscular mechanisms of wing beat in hummingbirds. *Z. Vgl. Physiol.* **60**, 209–218.
- Hedrick, T. L., Tobalske, B. W. and Biewener, A. A. (2003). How cockatiels (*Nymphicus hollandicus*) modulate pectoralis power output across flight speeds. *J. Exp. Biol.* **206**, 1363–1378.
- Reiser, P. J., Welch, K. C., Jr, Suarez, R. K. and Altshuler, D. L. (2013). Very low force-generating ability and unusually high temperature dependency in hummingbird flight muscle fibers. *J. Exp. Biol.* **216**, 2247–2256.
- Roberts, T. J. (2002). The integrated function of muscles and tendons during locomotion. *Comp. Biochem. Physiol.* **133A**, 1087–1099.
- Sokoloff, A. J., Gray-Chickering, J., Harry, J. D., Poore, S. O. and Goslow, G. E., Jr (2001). The function of the supracoracoideus muscle during takeoff in the European starling (*Sternus vulgaris*): Maxheinz Sy revisited. In *New Perspectives on the Origin and Early Evolution of Birds: Proceedings of the International Symposium in Honor of John H. Ostrom* (ed. J. H. Ostrom, J. Gauthier and L. F. Gall), pp. 319–332. New Haven: Peabody Museum of Natural History.
- Suarez, R. K. (1992). Hummingbird flight: sustaining the highest mass-specific metabolic rates among vertebrates. *Experientia* **48**, 565–570.
- Tobalske, B. W. (2010). Hovering and intermittent flight in birds. *Bioinspir. Biomim.* **5**, 045004.
- Tobalske, B. W. and Biewener, A. A. (2008). Contractile properties of the pigeon supracoracoideus during different modes of flight. *J. Exp. Biol.* **211**, 170–179.
- Tobalske, B. W. and Dial, K. P. (1994). Neuromuscular control and kinematics of intermittent flight in budgerigars (*Melopsittacus undulatus*). *J. Exp. Biol.* **187**, 1–18.

- Tobalske, B. W., Olson, N. E. and Dial, K. P.** (1997). Flight style of the black-billed magpie: variation in wing kinematics, neuromuscular control, and muscle composition. *J. Exp. Zool.* **279**, 313-329.
- Tobalske, B. W., Hedrick, T. L., Dial, K. P. and Biewener, A. A.** (2003). Comparative power curves in bird flight. *Nature* **421**, 363-366.
- Tobalske, B. W., Warrick, D. R., Clark, C. J., Powers, D. R., Hedrick, T. L., Hyder, G. A. and Biewener, A. A.** (2007). Three-dimensional kinematics of hummingbird flight. *J. Exp. Biol.* **210**, 2368-2382.
- Tobalske, B. W., Biewener, A. A., Warrick, D. R., Hedrick, T. L. and Powers, D. R.** (2010). Effects of flight speed upon muscle activity in hummingbirds. *J. Exp. Biol.* **213**, 2515-2523.
- Warrick, D. R., Tobalske, B. W. and Powers, D. R.** (2005). Aerodynamics of the hovering hummingbird. *Nature* **435**, 1094-1097.
- Warrick, D. R., Tobalske, B. W. and Powers, D. R.** (2009). Lift production in the hovering hummingbird. *Proc. Biol. Sci.* **276**, 3747-3752.
- Welch, K. C., Jr and Altshuler, D. L.** (2009). Fiber type homogeneity of the flight musculature in small birds. *Comp. Biochem. Physiol.* **152B**, 324-331.
- Wells, D. J.** (1993). Ecological correlates of hovering flight of hummingbirds. *J. Exp. Biol.* **178**, 59-70.
- Zusi, R. and Bentz, D.** (1984). Myology of purple-throated carib (*Eulampis jugularis*) and other hummingbirds (Aves: Trochilidae). *Smithson. Contrib. Zool.* **385**, 1-70.